

1 Rapid evolutionary diversification of the *flamenco* locus across simulans clade *Drosophila*
2 species

3

4

5

6

7

8 Sarah Signor^{1*}, Jeffrey Vedanayagam², Filip Wierzbicki^{3,4}, Robert Kofler³, and Eric C. Lai²

9

10

11

12 *Corresponding author: sarah.signor@ndsu.edu

13

14

15 ¹Biological Sciences, North Dakota State University, Fargo, North Dakota, USA

16 ²Developmental Biology Program, Sloan-Kettering Institute, 430 East 67th St, ROC-10, New

17 York, NY 10065, USA

18 ³Institut für Populationsgenetik, Vetmeduni Vienna, Vienna, Austria

19 ⁴Vienna Graduate School of Population Genetics, Vienna, Austria

20

21

22

23

24

25 **Abstract**

26 Effective suppression of transposable elements (TEs) is paramount to maintain genomic
27 integrity and organismal fitness. In *D. melanogaster*, *flamenco* is a master suppressor of TEs,
28 preventing their movement from somatic ovarian support cells to the germline. It is transcribed
29 by Pol II as a long (100s of kb), single-stranded, primary transcript, that is metabolized into
30 Piwi-interacting RNAs (piRNAs) that target active TEs via antisense complementarity. *flamenco*
31 is thought to operate as a trap, owing to its high content of recent horizontally transferred TEs
32 that are enriched in antisense orientation. Using newly-generated long read genome data, which
33 is critical for accurate assembly of repetitive sequences, we find that *flamenco* has undergone
34 radical transformations in sequence content and even copy number across *simulans* clade
35 Drosophilid species. *D. simulans flamenco* has duplicated and diverged, and neither copy
36 exhibits synteny with *D. melanogaster* beyond the core promoter. Moreover, *flamenco*
37 organization is highly variable across *D. simulans* individuals. Next, we find that *D. simulans*
38 and *D. mauritiana flamenco* display signatures of a dual-stranded cluster, with ping-pong signals
39 in the testis and embryo. This is accompanied by increased multicopy elements, consistent with
40 these regions operating as functional dual stranded clusters. Overall, the physical and functional
41 diversity of *flamenco* orthologs is testament to the extremely dynamic consequences of TE arms
42 races on genome organization, not only amongst highly related species, but even amongst
43 individuals.

44

45

46

47 **Introduction**

48 *Drosophila* gonads exemplify two important fronts in the conflict between transposable elements
49 (TEs) and the host – the germline (which directly generates gametes), and somatic support cells
50 (from which TEs can invade the germline) (1, 2). The strategies by which TEs are suppressed in
51 these settings are distinct (3), but share their utilization of piwi-interacting RNAs (piRNAs).
52 These are ~24-32 nt RNAs that are bound by the PIWI subclass of Argonaute proteins, and guide
53 them and associated cofactors to targets for transcriptional and/or post-transcriptional silencing
54 (4–7).

55 Mature piRNAs are processed from non-coding piRNA cluster transcripts, which derive
56 from genomic regions that are densely populated with TE sequences (7–9). However, the
57 mechanisms of piRNA biogenesis differ between gonadal cell types. In the germline, piRNA
58 clusters are transcribed from both DNA strands through non-canonical Pol II activity (6, 10–12),
59 which is initiated by chromatin marks rather than specific core promoter motifs. Moreover, co-
60 transcriptional processes such as splicing and polyadenylation are suppressed within dual strand
61 piRNA clusters (13, 14). On the other hand, in ovarian somatic support cells, piRNA clusters are
62 transcribed from a typical promoter as a single stranded transcript, which can be alternatively
63 spliced as with protein-coding mRNAs (15–18). These rules derive in large part from the study
64 of model piRNA clusters (i.e. the germline *42AB* and somatic *flamenco* piRNA clusters). For
65 both types, their capacity to repress invading transposable elements is thought to result from
66 random integration of new transposons into the cluster. As such, piRNA clusters are adaptive
67 loci that play central roles in the conflict between hosts and TEs.

68 The location and activity of germline piRNA clusters are stochastic and evolutionarily
69 dynamic, as there are many copies of TE families in different locations that may produce

70 piRNAs (9, 19). By contrast, somatic piRNA clusters are not redundant and a single insertion of
71 a TE into a somatic piRNA cluster should be sufficient to prevent that TE from further
72 transposition (18, 20). Thus, *flamenco* should contain only one copy per TE family (18), which is
73 true in the *flamenco* locus of *D. melanogaster* (18). *flamenco* is also the only piRNA cluster
74 which produces a phenotypic effect when altered, as germline clusters can be deleted with no
75 consequences.

76 *flamenco* has been a favored model for understanding the piRNA pathway since the
77 discovery of piRNA mediated silencing of transposable elements (6). *flamenco* spans >180 kb of
78 repetitive sequences located in β -heterochromatin of the X chromosome (21). Of note, *flamenco*
79 was initially identified, prior to the formal recognition of piRNAs, via transposon insertions that
80 de-repress *gypsy*, *ZAM*, and *Idefix* class elements (21–25). These mutant alleles disrupt the
81 *flamenco* promoter, and consequently abrogate transcription and piRNA production from this
82 locus. By contrast, the recent deletion of multiple model germline piRNA clusters, which
83 eliminate the biogenesis of a bulk of cognate piRNAs, did not de-repress their cognate TEs (9).
84 Thus, the analysis of *flamenco* evolution is presumably more consequential for TE dynamics.
85 Analysis of *flamenco* in various strains of *D. melanogaster* supports that this locus traps
86 horizontally derived TEs to achieve silencing of newly invaded TEs (18). The *flamenco* locus
87 exhibits synteny across the *D. melanogaster* sub-group (26); however, the sequence composition
88 of *flamenco* outside *D. melanogaster* has not been well-characterized (27).

89 In this study, we compare the *flamenco* locus across 10 strains of simulans-clade species,
90 namely *D. simulans*, *D. mauritiana*, and *D. sechellia*. Analysis of piRNAs from ovaries of five
91 genotypes of *D. simulans* found that *flamenco* is duplicated in *D. simulans*. This duplication is
92 old enough that there is no sequence synteny across copies, even though their core promoter

93 regions and the adjacent *dip1* gene are conserved. *flamenco* has also been colonized by abundant
94 (>40) copies of *RI*, a TE that was thought to insert only at ribosomal genes, and to evolve at the
95 same rate as nuclear genes [21]. Furthermore, between different genotypes, up to 63% of TE
96 insertions are not shared within any given copy of *flamenco*. Despite this, several full length TEs
97 are shared between all genotypes in a similar sequence context. This incredible diversity at the
98 *flamenco* locus, even within a single species, suggests there may be considerable variation in its
99 ability to suppress transposable elements across individuals.

100 Cross-species comparisons further indicate that functions of *flamenco* have diversified.
101 Data from *D. sechellia* and *D. melanogaster* conform with the current understanding of *flamenco*
102 as a uni-strand cluster. However, we find evidence that *D. simulans* and *D. mauritiana flamenco*
103 can act as a dual strand cluster in testis and embryos, yielding piRNAs from both strands with a
104 ping pong signal. Overall, we infer that the rapid evolution of *flamenco* alleles across individuals
105 and species reflects highly adaptive functions and dynamic biogenesis capacities.

106 **Materials and Methods**

107 *Fly strains*

108 The four *D. simulans* lines *SZ232*, *SZ45*, *SZ244*, and *SZ129* were collected in California from the
109 Zuma Organic Orchard in Los Angeles, CA on two consecutive weekends of February 2012 [57–
110 61]. *LNP-15-062* was collected in Zambia at the Luwangwa National Park by D. Matute and
111 provided to us by J. Saltz (J. Saltz pers. comm., [41,53]). *MD251*, *MD242*, *NS137*, and *NS40*
112 were collected in Madagascar and Kenya (respectively) and are described in [50]. The *D.*
113 *simulans* strain *wxD¹* was originally collected by M. Green, likely in California, but its
114 provenance has been lost (pers. comm. Jerry Coyne). *D. mauritiana (w12)* and *D. sechellia*
115 (*Rob3c/Tucson 14021-0248.25*) are described in [11].

116 *Long read DNA sequencing and assembly*

117 *MD242*, four SZ lines and *LNP-15-062* were sequenced on a MinION platform at North Dakota
118 State University (Oxford Nanopore Technologies (ONT), Oxford, GB), with base-calling using
119 guppy (v4.4.2). *MD242*, the four SZ lines, and *LNP-15-062* were assembled with Canu (v2.1)
120 [73] and two rounds of polishing with Racon (v1.4.3) [67]. The CA strains were additionally
121 polished with short reads using Pilon (v1.23) [68](SRR3585779, SRR3585440, SRR3585480,
122 SRR3585391) [60]. The first wxD^{I-1} assembly is described here [12]. *MD251*, *NS137*, *NS40* and
123 wxD^{I-2} were sequenced on a MinION platform by B. Kim at Stanford University. They were
124 assembled with Flye [29], and polished with a round of Medaka followed by a round of pilon
125 [68]. Following this contaminants were removed with blobtools
126 (<https://zenodo.org/record/845347>, [30]), soft masked with RepeatModeler and Repeatmasker
127 [22,64], then aligned to the wxD^I as a reference with Progressive Cactus [3]. The assemblies
128 were finished with reference based scaffolding using Ragout [28]. *D. mauritiana* and *D.*
129 *sechellia* were sequenced with PacBio and assembled with FALCON using default parameters
130 (<https://github.com/PacificBiosciences/FALCON>)[11].The *D. melanogaster* assembly is
131 described here (47). A summary of the assembly statistics is available in Supplementary Table 1.
132 The quality of cluster assembly was evaluated using CUSCO as described in (19, 48)
133 (Supplementary File 1).

134 *Short read sequencing and mapping*

135 Short read sequencing was performed by Beijing Genomics Institute (BGI) on approximately 50
136 dissected ovaries from adult female flies (*SZ45*, *SZ129*, *SZ232*, *SZ244*, *LNP-15-062*). Short read
137 libraries from 0-2 hour embryos were prepared from *D. melanogaster*, wxD^{I-2} , *D. sechellia*, and
138 *D. mauritiana* (SRAXXX) (49). Small RNA from testis is described in (50, 51). Libraries were

139 filtered for adapter contamination and short reads between 23-29 bp were retained for mapping
140 with fastp (52). The RNA was then mapped to their respective genomes using bowtie (v1.2.3)
141 and the following parameters (-q -v 1 -p 1 -S -a -m 50 --best --strata) (53, 54). The resulting bam
142 files were processed using samtools (55). To obtain unique reads the bam files were filtered for
143 reads with 1 mapping position. To obtain counts files with weighted mapping the bam files were
144 processed using Rsubreads and the featureCounts function (56).

145 *Defining and annotating piRNA clusters*

146 piRNA clusters were defined using proTRAC [52]. piRNA clusters were predicted with a
147 minimum cluster size of 1 kb (option “-clsize 1000”), a P value for minimum read density of
148 0.07 (option “-pdens 0.07”), a minimum fraction of normalized reads that have 1T (1U) or 10A
149 of 0.33 (option “-1Tor10A 0.33”) and rejecting loci if the top 1% of reads account for more than
150 90% of the normalized piRNA cluster read counts (option “-distr 1-90”), and a minimal fraction
151 of hits on the main strand of 0.25 (option “-clstrand 0.25”). Note that this ties the piRNA clusters
152 to their function such that participation in the ping pong pathway can be inferred from these
153 patterns. Clusters were annotated using RepeatMasker (v. 4.0.7) and the TE libraries described in
154 Chakraborty et al. (2019) [12,64]. The position of *flamenco* was also evaluated based off of the
155 position of the putative promoter, the *dip1* gene, and the enrichment of *gypsy* elements [24].
156 Fragmented annotations were merged to form TE copies with onecodetofindthemall [5].

157 Fragmented annotations were also manually curated, particularly because TEs not present in the
158 reference library often have their LTRs and internal sequences classified as different elements.

159 *Aligning the flamenco promoter region*

160 The region around the *flamenco* promoter was extracted from each genotype and species with
161 bedtools getfasta (61). Sequences were aligned with clustal-omega and converted to nexus

162 format (62). Trees were built using a GTR substitution model and gamma distributed rate
163 variation across sites (63). The markov chain monte carlo chains were run until the standard
164 deviation of split frequencies was below .01, around one million generations. The consensus
165 trees were generated using `sumt conformat=simple`. The resulting trees were displayed with the
166 R package `ape` (64).

167 *Detecting ping pong signals in the small RNA data*

168 Ping pong signals were detected using `pingpongpro` [66]. This program detects the presence of
169 RNA molecules that are offset by 10 nt, such that stacks of piRNA overlap by the first 10 nt from
170 the 5' end. These stacks are a hallmark of piRNA mediated transposon silencing. The algorithm
171 also takes into account local coverage and the presence of an adenine at the 10th position. The
172 output includes a z-score between 0 and 1, the higher the z-score the more differentiated the ping
173 pong stacks are from random local stacks.

174 **Results**

175 *flamenco* in the *D. simulans* clade

176 We identified *D. simulans flamenco* from several lines of evidence: piRNA cluster calls from
177 proTRAC, its location adjacent to divergently transcribed *dip1*, the existence of conserved core
178 *flamenco* promoter sequences, and enrichment of *gypsy* elements (Figure 1A-D); Supplementary
179 Table 2). The *flamenco* locus is at least 376 kb in *D. simulans*. This is an expansion compared
180 with *D. melanogaster*, where *flamenco* is only 156 kb (*Canton-S*). In *D. sechellia* *flamenco* is
181 363 kb, however in *D. mauritiana* the locus has expanded to at least 840 kb (Supplementary
182 Table 2). This is a large expansion, and it is possible that the entire region does not act as the
183 *flamenco* locus. However, evidence that it does include uniquely mapping piRNAs are found
184 throughout the region and *gypsy* enrichment is consistent with a *flamenco*-like locus

185 (Supplementary Figure 1). There are no protein coding genes within the region, and while the
186 neighboring genes on the downstream side of *flamenco* in *D. melanogaster* have moved in *D.*
187 *mauritiana* (CG40813- CG41562 at 21.5 MB), the following group of genes beginning with
188 CG14621 is present and flanks *flamenco* as it is annotated. Thus in *D. melanogaster* the borders
189 of *flamenco* are flanked by *dip1* upstream and CG40813 downstream, while in *D. mauritiana*
190 they are *dip1* upstream and CG14621 downstream. Between all species the *flamenco* promoter
191 and surrounding region, including the *dip1* gene, are alignable and conserved (Figure 1E).

192 *Structure of the flamenco locus*

193 *Structure of the flamenco locus*

194 *D. melanogaster flamenco* bears a characteristic structure, in which the majority of TEs
195 are gypsy-class elements in the antisense orientation (79% antisense orientation, 85% of which
196 are gypsy elements) (Figure 1D; Supplementary Table 3). This is true in both the *iso-1* and
197 *Canton-S* strains. In *D. simulans*, *flamenco* has been colonized by large expansions of *RI*
198 transposable element repeats such that on average the percent of antisense TEs is only 50% and
199 the percent of the locus comprised of LTR elements is 55%. However, 76% of antisense
200 insertions are LTR insertions, thus the underlying *flamenco* structure is apparent when the *RI*
201 insertions are disregarded (Figure 1D). In *D. mauritiana flamenco* is 71% antisense, and of those
202 antisense elements it is 85% LTRs. Likewise in *D. sechellia* 78% of elements are antisense, and
203 of those 81% are LTRs. *flamenco* retains the overall structure of a canonical *D. melanogaster*-
204 like *flamenco* locus in all of these species, however in *D. simulans* the nature of the locus is
205 somewhat altered by the abundant *RI* insertions (Figure 1D).

206 *flamenco* is duplicated in *D. simulans*

207 In *D. simulans*, we unexpectedly observed that *flamenco* is duplicated on the X
208 chromosome; the duplication was confirmed with PCR and a restriction digest (Supplementary
209 Table 4). These duplications are associated with a conserved copy of the putative *flamenco*
210 enhancer as well as copies of the *dip1* gene located proximal to *flamenco* in *D. melanogaster*
211 (Figure 1C, 2A). While it is unclear which copy is orthologous to *D. melanogaster flamenco*, all
212 *D. simulans* lines bear one copy that aligns across genotypes. We refer to this copy as *D.*
213 *simulans flamenco*, and the other copies as duplicates. Otherwise, *flamenco* duplicates do not
214 align with one another and lack synteny amongst their resident TEs. Possible evolutionary
215 scenarios are that the *flamenco* duplication occurred early in the *simulans* lineage, that the
216 clustered evolved very rapidly, or that the duplication encompassed only the promoter region and
217 was subsequently colonized by TEs (Figure 1C, 2A).

218 The *flamenco* duplicate is absent in the *D. simulans* reference strain, *w*⁵⁰¹, but present in
219 *wxD*¹, suggesting it was polymorphic or absent between the collection of these strains (or was
220 not assembled). The duplicate retains the structure of *flamenco*, with an average of 67% of TEs
221 in the antisense orientation in the duplication of *flamenco*, and 91% of the TEs in the antisense
222 orientation are LTRs. The duplicate of *flamenco* is less impacted by *RI*, with some genotypes
223 having as few as 8 *RI* insertions (Figure 2C).

224 *RI LINE elements at the flamenco locus*

225 *RI* elements are well-known to insert into rDNA genes, are transmitted vertically, and evolve
226 similarly as the genome background rate [21]. They have also been found outside of rDNA
227 genes, but only as fragments. However, as mentioned, *RI* elements are abundant within *flamenco*
228 loci in the *simulans* clade. Outside of *flamenco*, *RI* elements in *D. simulans* are distributed
229 according to expectation, with full length elements occurring only within rDNA (Supplementary

230 File 6). Within *flamenco*, most copies of *RI* occur as tandem duplicates, creating large islands of
231 fragmented *RI* copies (Figure 2A). They are on average 3.7% diverged from the reference *RI*
232 from *D. simulans*. Across individual *D. simulans* genomes, ~99 kb of *flamenco* loci consists of
233 *RI* elements, fully 26% of their average total length. *SZ45*, *LNP-15-062*, *NS40*, *MD251*, and
234 *MD242* contain 4-7 full length copies of *RI* in the sense orientation, even though all but *SZ45*
235 bear fragmented *RI* copies on the antisense strand. (The *SZ45 flamenco* assembly is incomplete).
236 As the antisense *RI* copies are expected to suppress *RI* transposition, *flamenco* may not suppress
237 these elements effectively.

238 In *D. mauritiana*, *flamenco* harbors abundant fragments or copies of *RI* (19 on the
239 reverse strand and 20 on the forward strand), and only one large island of *RI* elements. In total,
240 *D. mauritiana* contains 84 kb of *RI* sequence within *flamenco*. In *D. mauritiana* there are 8 full
241 length copies of *RI* at the *flamenco* locus, 7 in antisense, which are not obviously due to a
242 segmental or local duplication. Finally, we find that *D. sechellia flamenco* lacks full length
243 copies of *RI*, and it contains only 18 KB of *RI* sequence (16 fragments on the reverse strand).
244 Yet, all the copies are on the sense strand, which would not produce fragments that can suppress
245 *RI* TEs. Essentially the antisense copies of *RI* in *D. mauritiana* should be suppressing the TE,
246 but we see multiple full length antisense insertions, and *D. sechellia* has no antisense copies, but
247 we see no evidence for recent *RI* insertions. From this it would appear that whatever is
248 controlling the transposition of *RI* lies outside of *flamenco*.

249 The presence of long sense-strand *RI* elements within *flamenco* is a departure from
250 expectation [21,72]. There is no evidence of an rDNA gene within the *flamenco* locus that would
251 explain the insertion of *RI* elements there, nor is there precedence for the large expansion of *RI*

252 fragments within the locus. Furthermore, the suppression of *RI* transposition does not appear to
253 be controlled by *flamenco*.

254 *piRNA production from RI*

255 On average *RI* elements within the *flamenco* locus of *D. simulans* produce more piRNA
256 than any other TE within *flamenco* (Supplementary Table 6). *RI* reads mapping to the forward
257 strand constitute an average of 51% of the total piRNAs within the *flamenco* locus from the
258 maternal fraction, ovary, and testis using weighted mapping. The only exception is the ovarian
259 sample from *SZ232* which is a large outlier at only 5%. However reads mapping to the reverse
260 strand account for an average of 84% of the piRNA being produced from the strand in every
261 genotype and tissue – maternal fraction, testis, or ovary. If unique mapping is considered instead
262 of weighted these percentages are reduced by approximately 20%, which is to be expected given
263 that *RI* is present in many repeated copies. Production of piRNA from the reverse strand seems
264 to be correlated with elements inserted in the sense orientation, of which the vast majority are *RI*
265 elements in *D. simulans* (Supplementary Figure 2). The production of large quantities of piRNA
266 cognate to the *RI* element is seemingly pointless – if *RI* only inserts at rDNA genes and are
267 vertically transmitted there is little reason to be producing the majority of piRNA in response to
268 this element.

269 In *D. sechellia* there are very few piRNA produced from *flamenco* in these tissues, and
270 there are no full length copies of *RI*. Likewise overall weighted piRNA production from *RI*
271 elements on either strand is 2.8-5.9% of the total mapping piRNA. In contrast in *D. mauritiana*
272 there are full length *RI* elements and abundant piRNA production in the maternal fraction and
273 testis. In *D. mauritiana* an average of 28% of piRNAs mapping to the forward strand of *flamenco*
274 are arising from *RI*, and 33% from the reverse strand. In *D. mauritiana* *RI* elements make up a

275 smaller proportion of the total elements in the sense orientation (24%), versus *D. simulans*
276 (55%).

277 *Conservation of flamenco*

278 The *dip1* gene and promoter region adjacent to each copy of *flamenco* are very conserved both
279 within and between copies of *flamenco* (Figure 2). The phylogenetic tree of the area suggests that
280 we are correct in labeling the two copies as the original *flamenco* locus and the duplicate (Figure
281 2). The original *flamenco* locus is more diverged amongst copies while the duplicate clusters
282 closely together with short branch lengths (Figure 2). They are also conserved and alignable
283 between *D. melanogaster*, *D. sechellia*, *D. mauritiana*, and *D. simulans* (Figure 1). However, the
284 same is not true of the *flamenco* locus itself. Approximately 3 kb from the promoter *flamenco*
285 diverges amongst genotypes and species and is no longer alignable by traditional sequence-based
286 algorithms, as the TEs are essentially a presence/absence that spans multiple kb. There is no
287 conservation of *flamenco* between *D. melanogaster*, *D. simulans*, *D. sechellia*, and *D.*
288 *mauritiana* (Figure 3). However, within the *simulans* clade many of the same TEs occupy the
289 locus, suggesting that they are the current genomic invaders in each of these species (Figure 3).

290 In *D. simulans* the majority of full length TEs are singletons – 52% in *flamenco* and 64%
291 in the duplicate. Copies that are full length in one genotype but fragmented in others are counted
292 as shared, not singletons. Almost half of these singletons in the duplicate are due to a single
293 genotype with a unique section of sequence, in this case *MD251*. Likewise a third of the
294 singleton insertions in the duplicate are due to an *NS40* specific region of *flamenco*. Regardless
295 of these concentrations of singletons in single genotypes, it is the single largest category of
296 transposable element insertions, followed by fixed insertions. Thus even within a single
297 population there is considerable diversity at the *flamenco* locus, and subsequently diversity in the

298 ability to suppress transposable elements. For example, *gypsy-29* is present in three genotypes
299 either in *flamenco* or the duplicate, which would suggest that these genotypes are able to
300 suppress this transposable element in the somatic support cells of the ovary while the other
301 genotypes are not. In contrast *gypsy-3* is present in more than one full length copy in *flamenco*
302 and its duplicate in every genotype but one where it is present in a single copy. There are a
303 number of these conserved full length TEs that are present in all or nearly all genotypes,
304 including *Chimpo*, *gypsy-2*, *Tirant*, and *gypsy-4*. In addition, the *INE1* elements adjacent to the
305 promoter are always conserved.

306 It is notable that any full length TEs are shared across all genotypes, given that *wxD¹* was
307 like collected 30-50 years prior to the others, and the collections span continents (Figure 2). Two
308 facts are relevant to this observation: (1) TEs were shown not correlate with geography [32] and
309 (2) *D. simulans* is more diverse within populations than between different populations
310 [38,54,62]. Other explanations are also plausible. Selection could be maintaining these full
311 length TEs, *wxD¹* could have had introgression from other lab strains, or a combination of these
312 explanations.

313 *Suppression of TEs by the flamenco locus and the trap model of TE control*

314 In *D. melanogaster*, it was proposed that while germline clusters may have many insertions of a
315 single TE, the somatic 'master regulator' *flamenco* will have a single insertion of each
316 transposon, after which they are silenced and no longer able to transpose [72].

317 Here, we evaluate the following lines of evidence to determine if they support the trap model of
318 transposable element suppression. (1) How many TEs have antisense oriented multicopy
319 elements within *flamenco*? (2) How many TEs have full length and fragmented insertions,
320 suggesting the older fragments did not suppress the newer insertion? (3) How many *de novo*

321 insertions of TEs in the *flamenco* duplicate of *D. simulans* are also present in the original
322 *flamenco* copy?

323 How many TEs have antisense oriented multicopy elements within *flamenco*?

324 Due to the difficulty in classifying degraded elements accurately, for example between multiple
325 classes of *gypsy* element, we will focus here on full length TEs, suggesting recent transposition.

326 In *D. melanogaster* there are 7 full length elements, none of which are present in more than one
327 antisense copy. These elements make up 27% of the *flamenco* locus. Full length copies of five of
328 these elements were also reported previously for other strains of *D. melanogaster* (18)

329 In *D. sechellia* there are 14 full length TEs within the *flamenco* locus, three of which are
330 present in multiple copies. Two of these, *INE1* and *412*, are likely present due to local
331 duplication. In particular the *INE1* elements flank the promoter, are in the sense orientation, and
332 are conserved between *D. sechellia*, *D. mauritiana*, and *D. simulans*. The only element present in
333 multiple antisense copies is *GTWIN*. Similar to *D. melanogaster* these elements make up 27% of
334 the *flamenco* locus.

335 *D. mauritiana* contains 22 full length TEs within the *flamenco* locus. Four of these are
336 present in multiple antisense full length copies – *INE1*, *RI*, *Stalker-4*, and *Cr1a*. While some of
337 the five antisense copies of *RI* likely originated from local duplications – they are in the same
338 general region and tend to be flanked by *gypsy-8*, not all of them show these patterns.
339 Furthermore, as aforementioned, there also are full length sense copies of *RI* suggesting *RI* is
340 not being suppressed by *flamenco*. *gypsy-12* and *gypsy-3* have a second antisense copy within
341 *flamenco* that is just below the cutoff to be considered full length – in *gypsy-3* the second copy is
342 10% smaller, for *gypsy-12* it is 80% present but missing an LTR. Full length TEs make up 19%
343 of the *flamenco* locus.

344 In *D. simulans* there are 29 full length TEs present in any of the seven complete *flamenco*
345 assemblies. Eight of these are present in multiple antisense copies within a single genome –
346 *INE1*, *Chimpo*, *copia*, *gypsy-3*, *gypsy-4*, *412*, *Tirant*, and *BEL-unknown*. The two *Tirant* copies
347 are likely a segmental duplication as they flank an *RI* repeat region. In addition, most *INE1*
348 copies are present proximal to the promoter as aforementioned, however in *NS40* a copy is
349 present in antisense at the end of the locus. *Chimpo* is present in three full length copies within
350 *MD242 flamenco*, with no evidence of local duplication. While there are no full length copies of
351 *RI* inserted in antisense, *RI* is present in full length sense copies despite many genomes
352 containing antisense fragments, suggesting *flamenco* is not suppressing *RI*. On average full
353 length TEs constitute 20% of *flamenco* in *D. simulans*.

354 In the duplicate of *flamenco* in *D. simulans* there are 30 full length TEs present in any
355 one of the five complete *flamenco* duplicate assemblies. However, none of them are multicopy in
356 antisense. However, they are multicopy relative to the original copy of *flamenco*. *gypsy-3*, *BEL-*
357 *unknown*, *Nomad-1*, *Chimpo*, *gypsy-53A*, *RI*, and *INE1* are all multicopy with respect to the
358 original *flamenco* within a given genome. Some of these may have been inherited at the time of
359 duplication, however are full length in both copies suggesting recent transposition. In the
360 duplicate of *flamenco* full length TEs occupy an average of 17% of the locus. *MD251* is an
361 exception which weights the average, with 28% of the locus, while between 10 and 15% is found
362 for the remaining copies. Thus *D. simulans* and *D. mauritiana* overall do not meet the
363 expectation that *flamenco* will contain a single insertion of any given TE.

364 How many TEs have full length and fragmented insertions?

365 Full length elements are younger insertions than fragmented insertions. If a full length element is
366 inserted in *flamenco* and there are fragments in the antisense orientation elsewhere in *flamenco*
367 this indicates that *flamenco* did not successfully suppress the transposition of this element.

368 In *D. melanogaster* two elements have fragments in antisense and a full length TE – *Doc*
369 and *Stalker-2*. *D. sechellia* has 9 elements that are present as a full length TE and a fragment in
370 antisense (including *412*, *GTWIN*, *mdg-1*, and *nomad*) and 6 that are multicopy that are due to a
371 solo LTR (including *blood*, *297*, and *Stalker-4*). *D. mauritiana* has 21 elements that are present
372 in full length and a fragment in antisense (including *blood*, *412*, *gypsy-10-13*, and *R1*), and four
373 elements that are multicopy due to a solo LTR (*mdg-1*, *Idefix*, and *gypsy-7,10*).

374 In *D. simulans*, TEs that fit this criteria in *flamenco* include *gypsy-2*, *gypsy-3*, *gypsy-4*,
375 *gypsy-5*, *Chimpo*, *412*, *INE1*, *R1*, *Tirant*, and *Zam*. *297* and *Nomad-1* are present in full length
376 copies but only multi-copy in the context of solo LTRs. In the duplicate of *flamenco* in *D.*
377 *simulans* this includes *gypsy-2*, *gypsy-3*, *gypsy-5*, *297*, *Stalker-4*, and *R1*. For example in *NS40*
378 there are 7 full length copies of *R1* in the sense orientation that likely duplicated in place, as well
379 as 12 partial copies in the antisense orientation. In the *simulans* clade either fragments of TEs are
380 not sufficient to suppress transposable elements or some elements are able to transpose despite
381 the hosts efforts to suppress them.

382 *Is flamenco a trap for TEs entering through horizontal transfer?*

383 High sequence similarity between TEs in different species suggests horizontal transfer [36].
384 However, because sequence similarity can also exist due to vertical transmission we will use
385 sequence similarity between *R1* elements (inserted at rDNA genes) as a baseline for
386 differentiating horizontal versus vertical transfer. There has never been any evidence found for
387 horizontal transfer of *R1* and it is thought to evolve at the same rate as nuclear genes in the

388 *melanogaster* subgroup [21,72]. Of the full length elements present in any genome at *flamenco*
389 62% of them appear to have originated from horizontal transfer. This is similar to previous
390 estimates for *D. melanogaster* in other studies [72]. Transfer appears to have occurred primarily
391 between *D. melanogaster*, *D. sechellia*, and *D. willistoni*. This includes some known horizontal
392 transfer events such as *Chimpo* and *Chouto* [7], and others which have not been recorded such as
393 *gypys-29* (*D. willistoni*) and the *Max-element* (*D. sechellia*) (Supplemental File 3). The duplicate
394 of *flamenco* is similar, with 53% of full length TEs originating from horizontal transfer. They are
395 many of the same TEs, with a 46% overlap, thus *flamenco* and its duplicate are trapping many of
396 the same TEs. Both *flamenco* and the duplicate the region appears to serve as a trap for TEs
397 originating from horizontal transfer.

398 In *D. melanogaster* 85% of full length TEs appear to have arisen through horizontal
399 transfer, primarily with *D. yakuba* and *D. sechellia* [72]. In *D. sechellia* 53% of full length TEs
400 have arisen from horizontal transfer, including some known to have moved by horizontal transfer
401 such as *GTWIN* (*D. melanogaster/D. erecta*) [7]. *D. mauritiana* has 68% of its full length TEs
402 showing a closer relationship than expected by vertical descent with TEs from *D. sechellia*, *D.*
403 *melanogaster*, and *D. simulans*. The hypothesis that *flamenco* serves as a trap for TEs entering
404 the population through horizontal transfer holds throughout the *simulans* clade.

405 *Flamenco piRNA is expressed in the testis and the maternal fraction*

406 Canonically, *flamenco* piRNA is expressed in the somatic follicular cells of the ovary and
407 not in the germline, and also does not produce a ping pong signal [46]. It was not thought to be
408 present in the maternal fraction of piRNAs or other tissues. However, that appears to be variable
409 in different species (Figure 4). We examined single mapping reads in the *flamenco* region from
410 testes and embryos (maternal fraction) in *D. simulans*, *D. mauritiana*, *D. sechellia*, and *D.*

411 *melanogaster*. In *D. simulans* and *D. mauritiana flamenco* is expressed bidirectionally in the
412 maternal fraction and the testis, including ping pong signals on both strands (Figure 4). In *D.*
413 *sechellia*, there is no expression of *flamenco* in either of these tissues. Using weighted mapping
414 in the maternal fraction 63% (*D. mauritiana*) – 36% (*D. simulans*) of the ping pong signatures on
415 the X with a z-score of at least 0.9 are located within *flamenco* (Figure 4). Similar patterns are
416 seen in the testis, with 50% (*D. mauritiana*) to 40% (*D. simulans*) of ping pong signals on the X
417 with a z-score of at least 0.9 being located within *flamenco*. In *D. melanogaster*, there is uni-
418 strand expression in the maternal fraction, but it is limited to the region close to the promoter. In
419 *D. melanogaster* no ping pong signals have a z-score of 0.9, however of those with a z-score of
420 at least 0.8 only 2.3% of those on the X are potentially located within *flamenco*, suggesting that
421 the role of *flamenco* in these tissues has evolved between species.

422 In the duplicate of *flamenco* in the maternal fraction 18% of the ping pong signals on the
423 X are within the *flamenco* duplicate, while in the testis this is 13%. While overall expression of
424 unique piRNAs is lower, proportionally the locus appears to behave the same in each tissue as
425 the original copy of *flamenco*. In addition, *flamenco* in these species has been colonized by full
426 length TEs thought to be germline TEs such as *blood*, *burdock*, *mdg-3*, *Transpac*, and *Bel*
427 [16,20]. *blood* is also present in *D. melanogaster* in a full length copy while there is no evidence
428 of germline activity for *flamenco* in *D. melanogaster*, though no other putative germline
429 *Silencing of transposable elements*

430 **Discussion**

431 The piRNA pathway is the organisms primary mechanism of transposon suppression.
432 While the piRNA pathway is conserved, the regions of the genome that produce piRNA are
433 labile, particularly in double stranded germline piRNA clusters [23]. The necessity of any single

434 cluster for TE suppression in the germline piRNA pathway is unclear, but likely redundant [23].
435 However, *flamenco* is thought to be the master regulator of the somatic support cells of the
436 ovary, preventing *gypsy* elements from hopping into germline cells [19,42,45,46,48,72]. It is not
437 redundant to other clusters, and insertion of a single element into *flamenco* in *D. melanogaster* is
438 sufficient to initiate silencing. Here we show that the function of *flamenco* appears to have
439 diversified in the *D. simulans* clade, acting in at least some tissues as a germline piRNA cluster.

440 *Dual stranded expression of flamenco*

441 In this work, we showed that piRNAs of the *flamenco* locus in *D. simulans* and *D.*
442 *mauritiana* are deposited maternally, align to both strands, and exhibit ping-pong signatures.
443 This is in contrast to *D. melanogaster*, where *flamenco* acts as a uni-strand cluster in the soma
444 [40], our data thus suggest that the *flamenco* locus in *D. simulans* and *D. mauritiana* acts as a
445 dual-strand cluster in the germline. In *D. sechellia* the attributes of *flamenco* uncovered in *D.*
446 *melanogaster* appear to be conserved – no expression in the maternal fraction and the testis and
447 no ping pong signals. Given that *flamenco* is likely a somatic uni-strand cluster in *D. erecta*, we
448 speculate that the conversion into a germline cluster happened in the *simulans* clade [40]. Such a
449 conversion of a cluster between the somatic and the germline piRNA pathway is not
450 unprecedented. For example, a single insertion of a reporter transgene triggered the conversion
451 of the uni-stranded cluster *20A* in *D. melanogaster* into a dual-strand cluster [37].

452 The role of *flamenco* in *D. simulans* and *D. mauritiana* as the master regulator of piRNA
453 in somatic support cells may still well be true – the promoter region of the *flamenco* cluster is
454 conserved between species and between copies of *flamenco* within species. This suggests that in
455 at least some contexts (or all) the cluster is still serving as a unistrand cluster transcribed from a
456 traditional RNA Pol II site [24]. However it has acquired additional roles, producing dual strand

457 piRNA and ping pong signals, in these two species, in at least the germline and testis. However,
458 in *D. simulans*, the majority of these reverse stranded piRNAs are emerging from the *RI*
459 insertions within *flamenco*. There is no evidence at present that *RI* has undergone an expansion
460 in function in *D. simulans*, thus it is unclear what, if any, functional impact the reverse stranded
461 piRNAs have at the *flamenco* locus.

462 *Duplication of flamenco in D. simulans*

463 In *D. simulans*, *flamenco* is present in 2-3 genomic copies, and this duplication is present
464 in all sequenced *D. simulans* lines. The *dip1* gene and putative *flamenco* promoter flanking the
465 duplication also has a high similarity in all sequenced lines (Fig. 2B). This raises the possibility
466 that the duplication of *flamenco* in *D. simulans* was positively selected. Such a duplication may
467 be beneficial as it increases the ability of an organism to rapidly silence TEs. Individuals with
468 large piRNA clusters (or duplicated ones) will accumulate fewer deleterious TE insertions than
469 individuals with small clusters (or non-duplicated ones), and duplicated clusters may therefore
470 confer a selective advantage [27].

471 *Rapid evolution of piRNA clusters*

472 A previous work showed that dual- and uni-strand clusters evolve rapidly in *Drosophila*
473 [70]. In agreement with this work we also found that the *flamenco*-locus is rapidly evolving
474 between and within species (Fig. 1C, 3B). A major open question remains whether this rapid
475 turnover is driven by selection (positive or negative) or an outcome of neutral processes (eg. high
476 TE activity or insertion bias of TEs). These rapid evolutionary changes at the *flamenco* locus, a
477 piRNA master locus, suggest that there is a constant turnover in patterns of piRNA biogenesis
478 that potentially leads to changes in the level of transposition control between individuals in a
479 population.

480

481

482 Funding

483 This work was supported by the National Science Foundation Established Program to Stimulate
 484 Competitive Research (NSF-EPSCoR-1826834 and NSF-EPSCoR-2032756)
 485 to SS and the Austrian Science Fund FWF (<https://www.fwf.ac.at/>;) grant P35093 to RK. J.V. was
 486 supported by a Pathway to Independence award from the National Institute of General Medical
 487 Sciences (K99-GM137077). E.C.L. was supported by the National Institute of General Medical
 488 Sciences (R01-GM083300) and National Institutes of Health MSK Core Grant (P30-CA008748).
 489

490

491

492 Competing interests

493 We declare that we have no competing interests.
 494

495

496 Acknowledgements

497 S.S. would like to thank C. & F. & S. Emery for insightful commentary on the manuscript.
 498

499

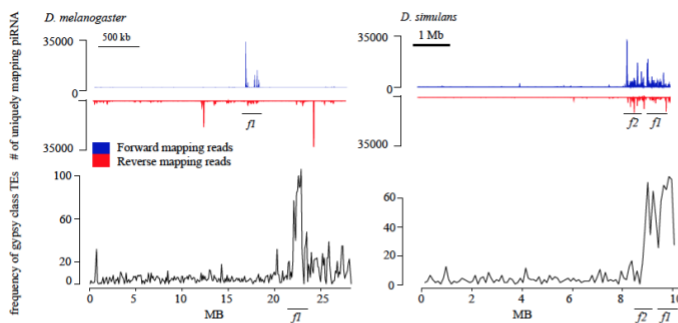
500 Authors' contributions

501 S.S. conceived the study, performed bioinformatics and drafted portions of the manuscript. FW
 502 and RK performed bioinformatics and drafted portions of the manuscript. JV contributed data
 503 and bioinformatic analysis. EL drafted portions of the manuscript and provided data.
 504

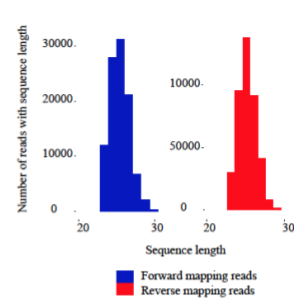
505 Availability of data and materials

All data has been made available in the following repositories:

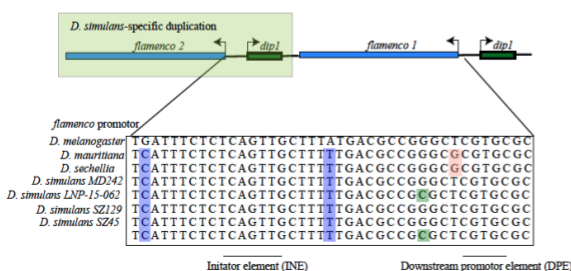
A Uniquely mapping piRNA and gypsy enrichment in the flamenco area of *D. melanogaster* and *D. simulans*



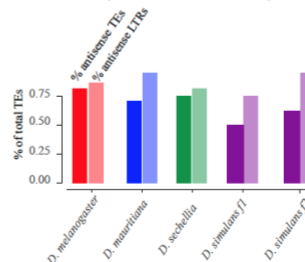
B Distribution of read lengths mapping to flamenco in *D. simulans*



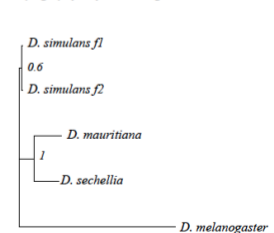
C The flamenco region in the simulans clade



D Enrichment of antisense elements and LTRs in flamenco



E Phylogeny of the flamencoc region



505

506

507 **Figure 1.** A) Unique piRNA from the ovary and *gypsy* enrichment around *flamenco* and its
508 duplicate in *D. simulans* and *D. melanogaster*. piRNA mapping to the entire contig that contains
509 *flamenco* is shown for both species. The top of the panel shows piRNA mapping to *flamenco* and
510 is split by antisense (blue) and sense (red) piRNA . The bottom panel shows the frequency of
511 *gypsy*-type transposon annotations across the contig containing *flamenco*, counted in 100 kb
512 windows. There is a clear enrichment of *gypsy* in the area of *flamenco* and, in *D. simulans*, its
513 duplicate compared to the rest of the contig. B) The distribution of read size for small RNA
514 mapping to *flamenco*. The peak is at approximately 26 bp, within the expected range for piRNA.
515 C) The duplication of *flamenco* in the *D. simulans*. Both copies are flanked by the *dip1* gene and
516 copies of the putative *flamenco* promoter. Polymorphisms within the promoter that are shared
517 within the *simulans* clade are shown in blue, *D. simulans* specific polymorphisms are shown in
518 green. The region around the promoter is very conserved across species. D) The percent of TEs
519 in *flamenco* in each species which are in the antisense orientation (first bar) and the percent of
520 TEs in the antisense orientation that are also LTR class elements (second bar). E) A phylogenetic
521 tree of the *dip1* and *flamenco* enhancer region for *D. melanogaster* and the *simulans* clade. This
522 region is conserved and alignable between all species. The tree was generated with Mr. Bayes
523 [51].

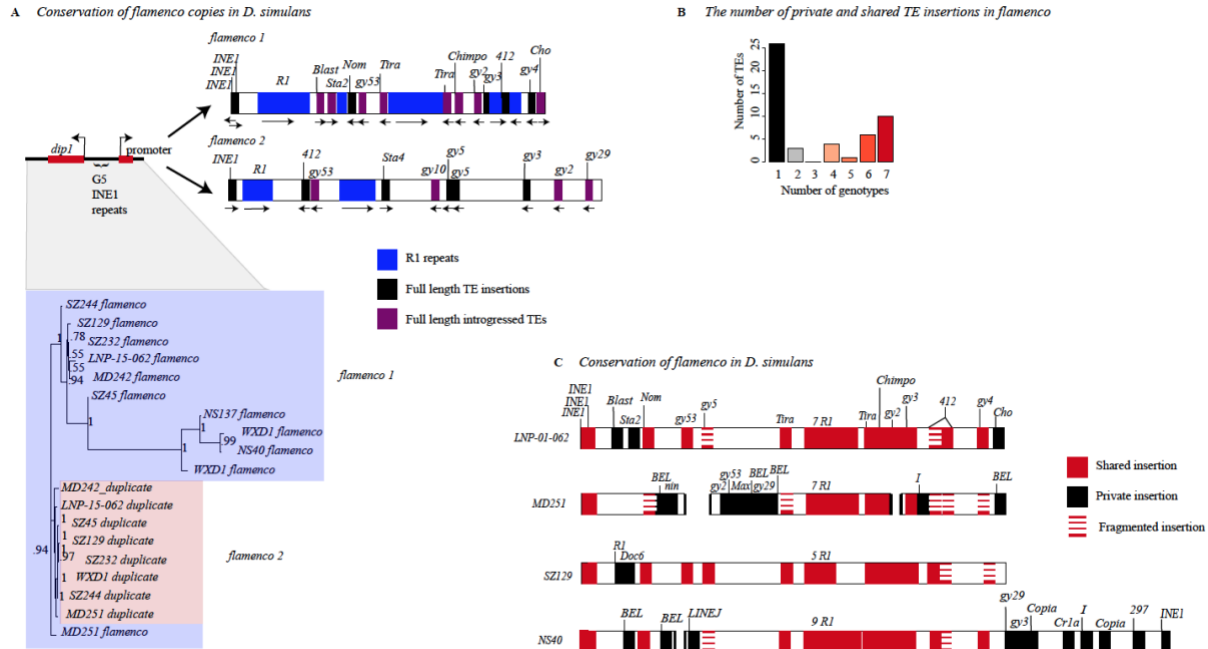
524

525

526

527

528



529
530
531

532

533 Figure 2. A) Divergence between copies of flamenco. Proximal is a phylogenetic tree of *dip1* and

534 the *flamenco* promoter region from each genome. In between *dip1* and the promoter are a series

535 of *G5/INE1* repeats that are found in every genome. Overall this region is fairly conserved, with

536 the duplicate copies all grouping together with short branch lengths (shown in pink). The original

537 copy of *flamenco* is more diverse with some outliers (shown in light blue) but there is good

538 branch support for all the deep branches of the tree. Distal is a representation of *flamenco* and its

539 duplicate. R1 repeat regions are shown in blue. Full length transposable elements are labeled.

540 There is no synteny conservation between *flamenco* and its duplicate. B) The proportion of

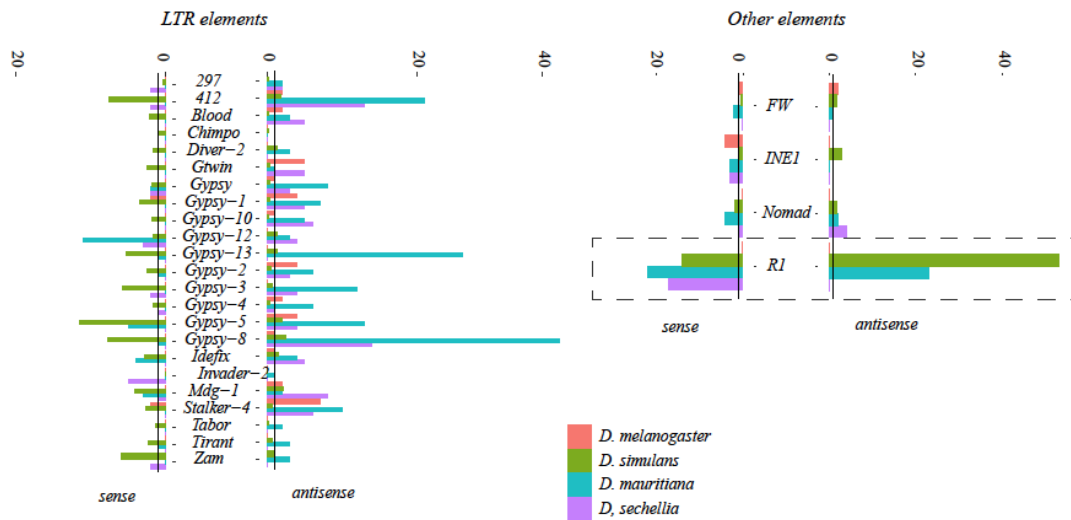
541 insertions that are shared by one through seven genotypes (genotypes with complete *flamenco*

542 assemblies). C) Divergence of flamenco within *D. simulans*. Labeled TEs correspond to

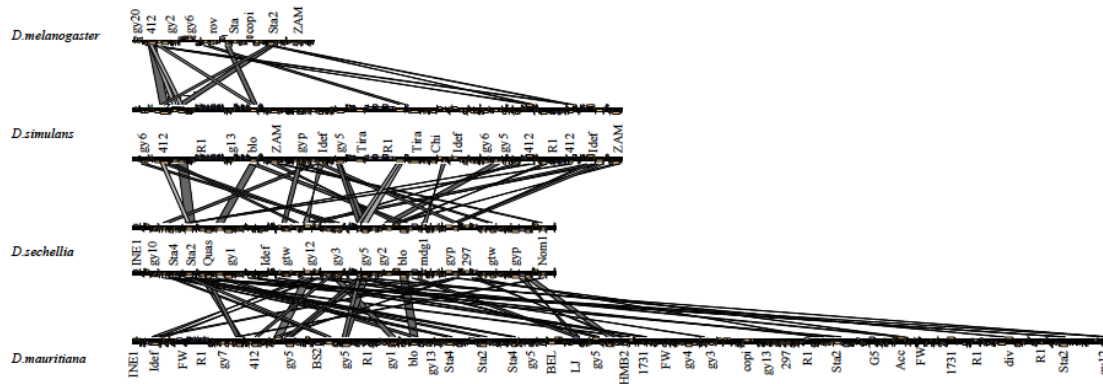
543 elements which are present in a full length copy in at least one genome. If they are shared

544 between genomes they are labeled in red, if they are unique they are black. If they are full length
 545 in one genome and degraded in other genomes they are represented by stacked dashes. If they are
 546 present in the majority of genomes but missing in one, it is represented as a missing that TE,
 547 which is agnostic to whether it is a deletion or the element was never present
 548
 549

A Copy number of a subset of TEs in the simulans clade



B Similarity of TEs in flamenco within the simulans clade



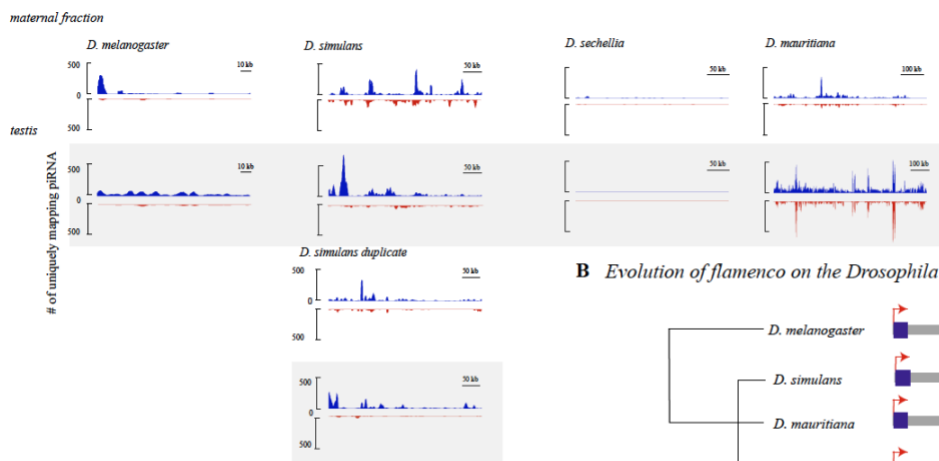
550

551

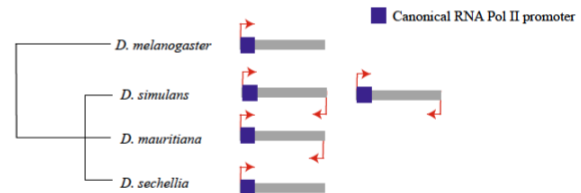
552

553 **Figure 3) A.** Copy number of a subset of transposable elements at *flamenco*. Solo LTRs are
 554 indicated by in a lighter shade at the top of the bar. The black line on each bar graph indicates a
 555 copy number of one. Values for *D. simulans* are the average for all genotypes with a complete
 556 *flamenco* assembly. Note that in *D. melanogaster* (green) most TEs have a low copy number.
 557 The expansion of *R1* elements in the *simulans* clade is clearly indicated on the right hand panel
 558 with a dotted box. Many elements within *flamenco* are multicopy in the *simulans* clade. While
 559 some of this is likely due to local duplications it is clearly a different pattern than *D.*
 560 *melanogaster*. Enrichment of LTR elements on the antisense strand is clear for all species. **B.**
 561 Alignment of *flamenco* in *D. melanogaster*, *D. simulans*, *D. sechellia*, and *D. mauritiana*. There
 562 is no conserved synteny between species but there are clearly shared TEs, particularly within the
 563 *simulans* clade. The expansion of *D. mauritiana* compared to the other species is apparent.

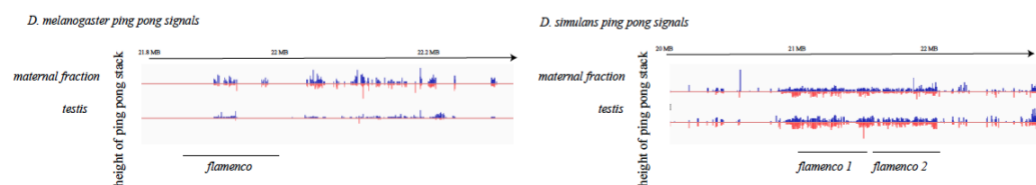
A Uniquely mapping piRNAs in the *simulans* clade



B Evolution of *flamenco* on the *Drosophila* phylogeny



C pingpong signals at *flamenco* in *D. melanogaster* and *D. simulans*



564 **Figure 4) A.** Expression of single mapping piRNAs in the maternal fraction and testis (gray) of
 565 *D. melanogaster* and the *simulans* clade. Antisense mapping reads are shown in blue, sense in
 566
 567

568 red. Libraries are RPM normalized and scaled across library type. *D. sechellia* has no expression
569 of *flamenco* in the maternal fraction or the testis. *D. melanogaster* has low expression in the
570 maternal fraction and very little ping pong activity. *D. simulans* and *D. mauritiana* show dual
571 stranded expression in the testis and maternal fraction. **B.** A schematic of the evolution of
572 *flamenco* and its mode expression in the *simulans* and *melanogaster* clade. **C.** *D. simulans* and
573 *D. mauritiana* (Supplementary File) have ping pong singles at *flamenco* in the testis and
574 maternal fraction, while *D. melanogaster* does not.

575

576

577

578

579 1. C. Duc, *et al.*, Trapping a somatic endogenous retrovirus into a germline piRNA cluster
580 immunizes the germline against further invasion. *Genome Biol* 20, 127 (2019).

581 2. B. Barckmann, *et al.*, The somatic piRNA pathway controls germline transposition over
582 generations. *Nucleic Acids Res* 46, gky761- (2018).

583 3. C. D. Malone, *et al.*, Specialized piRNA Pathways Act in Germline and Somatic Tissues of
584 the *Drosophila* Ovary. *Cell* 137, 522–535 (2009).

585 4. L. S. Gunawardane, *et al.*, A Slicer-Mediated Mechanism for Repeat-Associated siRNA 5'
586 End Formation in *Drosophila*. *Science* 315, 1587–1590 (2007).

587 5. S. H. Wang, S. C. R. Elgin, *Drosophila* Piwi functions downstream of piRNA production
588 mediating a chromatin-based transposon silencing mechanism in female germ line. *Proc*
589 *National Acad Sci* 108, 21164–21169 (2011).

590 6. J. Brennecke, *et al.*, Discrete Small RNA-Generating Loci as Master Regulators of Transposon
591 Activity in *Drosophila*. *Cell* 128, 1089–1103 (2007).

592 7. A. A. Aravin, *et al.*, The Small RNA Profile during *Drosophila melanogaster* Development.
593 *Developmental Cell* 5, 337–350 (2003).

594 8. G. Chirn, *et al.*, Conserved piRNA Expression from a Distinct Set of piRNA Cluster Loci in
595 Eutherian Mammals. *Plos Genet* 11, e1005652 (2015).

- 596 9. D. Gebert, *et al.*, Large *Drosophila* germline piRNA clusters are evolutionarily labile and
597 dispensable for transposon regulation. *Mol Cell* 81, 3965–3978.e5 (2021).
- 598 10. P. R. Andersen, L. Tirian, M. Vunjak, J. Brennecke, A heterochromatin-dependent
599 transcription machinery drives piRNA expression. *Nature* 549, 54–59 (2017).
- 600 11. C. Klattenhoff, *et al.*, The *Drosophila* HP1 Homolog Rhino Is Required for Transposon
601 Silencing and piRNA Production by Dual-Strand Clusters. *Cell* 138, 1137–1149 (2009).
- 602 12. F. Mohn, G. Sienski, D. Handler, J. Brennecke, The Rhino-Deadlock-Cutoff Complex
603 Licenses Noncanonical Transcription of Dual-Strand piRNA Clusters in *Drosophila*. *Cell* 157,
604 1364–1379 (2014).
- 605 13. Y.-C. A. Chen, *et al.*, Cutoff Suppresses RNA Polymerase II Termination to Ensure
606 Expression of piRNA Precursors. *Mol Cell* 63, 97–109 (2016).
- 607 14. F. Mohn, G. Sienski, D. Handler, J. Brennecke, The Rhino-Deadlock-Cutoff Complex
608 Licenses Noncanonical Transcription of Dual-Strand piRNA Clusters in *Drosophila*. *Cell* 157,
609 1364–1379 (2014).
- 610 15. C. Goriaux, S. Desset, Y. Renaud, C. Vaury, E. Brasset, Transcriptional properties and
611 splicing of the flamencopi RNA cluster. *EMBO reports* 15, 411–418 (2014).
- 612 16. G. Sienski, D. Dönertas, J. Brennecke, Transcriptional Silencing of Transposons by Piwi and
613 Maelstrom and Its Impact on Chromatin State and Gene Expression. *Cell* 151, 964–980 (2012).
- 614 17. C. Dennis, E. Brasset, C. Vaury, flam piRNA precursors channel from the nucleus to the
615 cytoplasm in a temporally regulated manner along *Drosophila* oogenesis. *Mobile DNA* 10, 203–9
616 (2019).
- 617 18. V. Zanni, A. Eymery, M. C. P. of the, 2013, Distribution, evolution, and diversity of
618 retrotransposons at the flamenco locus reflect the regulatory properties of piRNA clusters.
619 *National Acad Sciences* <https://doi.org/10.1073/pnas.1313677110/-/dcsupplemental>.
- 620 19. F. Wierzbicki, R. Kofler, S. Signor, Evolutionary dynamics of piRNA clusters in *Drosophila*.
621 *Mol Ecol* (2021) <https://doi.org/10.1111/mec.16311>.
- 622 20. C. M. Bergman, H. Quesneville, D. Anxolabéhère, M. Ashburner, Recurrent insertion and
623 duplication generate networks of transposable element sequences in the *Drosophila melanogaster*
624 genome. *Genome Biology* 7, R112–21 (2006).
- 625 21. N. Prud'homme, M. Gans, M. Masson, C. Terzian, A. Bucheton, Flamenco, a gene
626 controlling the gypsy retrovirus of *Drosophila melanogaster*. *Genetics* 139, 697–711 (1995).

- 627 22. S. U. Song, T. Gerasimova, M. Kurkulos, J. D. Boeke, V. G. Corces, An env-like protein
628 encoded by a Drosophila retroelement: evidence that gypsy is an infectious retrovirus. *Genes &*
629 *development* 8, 2046–2057 (1994).
- 630 23. M. Mével-Ninio, A. Pelisson, J. Kinder, A. R. Campos, A. Bucheton, The flamenco Locus
631 Controls the gypsy and ZAM Retroviruses and Is Required for Drosophila Oogenesis. *Genetics*
632 175, 1615–1624 (2007).
- 633 24. A. Pelisson, *et al.*, Gypsy transposition correlates with the production of a retroviral
634 envelope-like protein under the tissue-specific control of the Drosophila flamenco gene. *The*
635 *EMBO Journal* 13, 4401–4411 (1995).
- 636 25. A. Bucheton, The relationship between the flamenco gene and gypsy in Drosophila: how to
637 tame a retrovirus. *Trends Genet* 11, 349–353 (1995).
- 638 26. C. D. Malone, G. J. Hannon, Molecular Evolution of piRNA and Transposon Control
639 Pathways in Drosophila. *Cold Spring Harbor Symposia on Quantitative Biology* 74, 225–234
640 (2010).
- 641 27. A. G. Clark, *et al.*, Evolution of genes and genomes on the Drosophila phylogeny. *Nature*
642 450, 203–218 (2007).
- 643 28. D. G. Eickbush, W. C. Lathe, M. P. Francino, T. H. Eickbush, R1 and R2 retrotransposable
644 elements of Drosophila evolve at rates similar to those of nuclear genes. *Genetics* 139, 685–695
645 (1995).
- 646 29. S. A. Signor, F. N. New, S. Nuzhdin, A Large Panel of Drosophila simulans Reveals an
647 Abundance of Common Variants. *Genome Biology and Evolution* 10, 189–206 (2017).
- 648 30. S. Signor, S. Nuzhdin, Dynamic changes in gene expression and alternative splicing mediate
649 the response to acute alcohol exposure in Drosophila melanogaster. *Heredity* (2018).
- 650 31. S. Signor, Population genomics of Wolbachia and mtDNA in Drosophila simulans from
651 California. *Scientific Reports*, 1–11 (2017).
- 652 32. S. A. Signor, M. Abbasi, P. Marjoram, S. V. Nuzhdin, Social effects for locomotion vary
653 between environments in Drosophila melanogaster females. *Evolution* 71, 1765–1775 (2017).
- 654 33. S. Signor, Transposable elements in individual genotypes of Drosophila simulans. *Ecology*
655 *and Evolution* 130, 499–11 (2020).
- 656 34. D. R. Matute, J. Gavin-Smyth, G. Liu, Variable post-zygotic isolation in Drosophila
657 melanogaster/D. simulans hybrids. *Journal of Evolutionary Biology* 27, 1691–1705 (2014).

- 658 35. D. R. Schrider, J. Ayroles, D. R. Matute, A. D. Kern, Supervised machine learning reveals
659 introgressed loci in the genomes of *Drosophila simulans* and *D. sechellia*. *PLoS Genetics* 14,
660 e1007341-29 (2018).
- 661 36. R. L. Rogers, *et al.*, Landscape of Standing Variation for Tandem Duplications in *Drosophila*
662 *yakuba* and *Drosophila simulans*. *Molecular Biology and Evolution* 31, 1750–1766 (2014).
- 663 37. M. Chakraborty, *et al.*, Evolution of genome structure in the *Drosophila simulans* species
664 complex. *Genome Res.* 30, 1067–63 (2020).
- 665 38. , *Genome Res.* 2017-Koren-gr.215087.116.
- 666 39. R. Vaser, I. Sović, N. Nagarajan, M. Šikić, Fast and accurate de novo genome assembly from
667 long uncorrected reads. *Genome Res* 27, 737–746 (2017).
- 668 40. B. J. Walker, *et al.*, Pilon: An Integrated Tool for Comprehensive Microbial Variant
669 Detection and Genome Assembly Improvement. *Plos One* 9, e112963 (2014).
- 670 41. M. Kolmogorov, J. Yuan, Y. Lin, P. A. Pevzner, Assembly of long, error-prone reads using
671 repeat graphs. *Nat Biotechnol* 37, 540–546 (2019).
- 672 42. D. R. Laetsch, M. L. Blaxter, BlobTools: Interrogation of genome assemblies.
673 *F1000research* 6, 1287 (2017).
- 674 43. M. Tarailo-Graovac, N. Chen, Using RepeatMasker to Identify Repetitive Elements in
675 Genomic Sequences. *Current Protocols in Bioinformatics*, 1–14 (2009).
- 676 44. J. M. Flynn, *et al.*, RepeatModeler2 for automated genomic discovery of transposable
677 element families. *Proc National Acad Sci* 117, 9451–9457 (2020).
- 678 45. J. Armstrong, *et al.*, Progressive Cactus is a multiple-genome aligner for the thousand-
679 genome era. *Nature* 587, 246–251 (2020).
- 680 46. M. Kolmogorov, *et al.*, Chromosome assembly of large and complex genomes using multiple
681 references. *Genome Res* 28, 1720–1732 (2018).
- 682 47. F. Wierzbicki, F. Schwarz, O. Cannalunga, R. Kofler, Generating high quality assemblies for
683 genomic analysis of transposable elements. *Biorxiv*, 2020.03.27.011312 (2020).
- 684 48. F. Wierzbicki, F. Schwarz, O. Cannalunga, R. Kofler, Novel quality metrics allow
685 identifying and generating high-quality assemblies of piRNA clusters. *Mol Ecol Resour* 22, 102–
686 121 (2022).
- 687 49. Vedanayagam, Jeffrey, “Evolutionary Genomics of piRNA Mediated Transposon Silencing
688 in *Drosophila*,” University of Rochester. (2016).

- 689 50. J. Vedanayagam, *et al.*, Endogenous RNAi silences a burgeoning sex chromosome arms race.
690 *Biorxiv*, 2022.08.22.504821 (2022).
- 691 51. J. Vedanayagam, C.-J. Lin, E. C. Lai, Rapid evolutionary dynamics of an expanding family
692 of meiotic drive factors and their hpRNA suppressors. *Nat Ecol Evol* 5, 1613–1623 (2021).
- 693 52. S. Chen, Y. Zhou, Y. Chen, J. Gu, fastp: an ultra-fast all-in-one FASTQ preprocessor.
694 *Biorxiv*, 274100 (2018).
- 695 53. M. J. Axtell, ShortStack: Comprehensive annotation and quantification of small RNA genes.
696 *RNA* 19, 740–751 (2013).
- 697 54. B. Langmead, C. Trapnell, M. Pop, S. L. Salzberg, Ultrafast and memory-efficient alignment
698 of short DNA sequences to the human genome. *Genome Biol* 10, R25 (2009).
- 699 55. H. Li, *et al.*, The Sequence Alignment/Map format and SAMtools. *Bioinformatics* 25, 2078–
700 2079 (2009).
- 701 56. Y. Liao, G. K. Smyth, W. Shi, The R package Rsubread is easier, faster, cheaper and better
702 for alignment and quantification of RNA sequencing reads. *Nucleic Acids Res* 47, gkz114-
703 (2019).
- 704 57. H. Li, Minimap2: pairwise alignment for nucleotide sequences. *Genome Biology* 34, 3094–
705 3100.
- 706 58. D. Rosenkranz, H. Zischler, proTRAC - a software for probabilistic piRNA cluster detection,
707 visualization and analysis. *Bmc Bioinformatics* 13, 5 (2012).
- 708 59. M. Chakraborty, J. J. Emerson, S. J. Macdonald, A. D. Long, Structural variants exhibit
709 widespread allelic heterogeneity and shape variation in complex traits. *Nature Communications*,
710 1–11 (2019).
- 711 60. M. Bailly-Bechet, A. Haudry, E. Lerat, “One code to find them all”: a perl tool to
712 conveniently parse RepeatMasker output files. *Mobile Dna-uk* 5, 13 (2014).
- 713 61. A. R. Quinlan, I. M. Hall, BEDTools: a flexible suite of utilities for comparing genomic
714 features. *Bioinformatics* 26, 841–842 (2010).
- 715 62. F. Sievers, D. G. Higgins, Clustal Omega for making accurate alignments of many protein
716 sequences. *Protein Sci* 27, 135–145 (2018).
- 717 63. F. Ronquist, *et al.*, MrBayes 3.2: Efficient Bayesian Phylogenetic Inference and Model
718 Choice Across a Large Model Space. *Systematic Biology* 61, 539–542 (2012).
- 719 64. E. Paradis, J. Claude, K. Strimmer, APE: Analyses of Phylogenetics and Evolution in R
720 language. *Bioinformatics* 20, 289–290 (2004).

- 721 65. S. Uhrig, H. Klein, PingPongPro: a tool for the detection of piRNA-mediated transposon-
722 silencing in small RNA-Seq data. *Bioinformatics* 35, 335–336 (2018).
- 723 66. E. Lerat, *et al.*, Population specific dynamics and selection patterns of transposable element
724 insertions in European natural populations. *Molecular Ecology*, 1–42 (2018).
- 725 67. R. S. Singh, Population genetics and evolution of species related to *Drosophila melanogaster*.
726 *Annual Review of Genetics* 23, 425–453 (1989).
- 727 68. H. E. Machado, *et al.*, Comparative population genomics of latitudinal variation in
728 *Drosophila simulans* and *Drosophila melanogaster*. *Molecular Ecology* 25, 723–740 (2016).
- 729 69. A. Sedghifar, P. Saelao, D. J. Begun, Genomic patterns of geographic differentiation in
730 *Drosophila simulans*. *Genetics* (2016) <https://doi.org/10.1534/genetics.115.185496>.
- 731 70. D. A. Petrov, DNA loss and evolution of genome size in *Drosophila*. *Genetica* 115, 81–91
732 (2002).
- 733 71. E. L. S. Loreto, C. M. A. Carareto, P. Capy, Revisiting horizontal transfer of transposable
734 elements in *Drosophila*. *Heredity* 100, 545–554 (2008).
- 735 72. N. Bargues, E. Lerat, Evolutionary history of LTR-retrotransposons among 20 *Drosophila*
736 species. *Mobile Dna-uk* 8, 7 (2017).
- 737 73. Z. Durdevic, R. S. Pillai, A. Ephrussi, Transposon silencing in the *Drosophila* female
738 germline is essential for genome stability in progeny embryos. *Life Sci Alliance* 1, e201800179
739 (2018).
- 740 74. B. Czech, J. B. Preall, J. McGinn, G. J. Hannon, A Transcriptome-wide RNAi Screen in the
741 *Drosophila* Ovary Reveals Factors of the Germline piRNA Pathway. *Mol Cell* 50, 749–761
742 (2013).
- 743 75. G. Coline, E. Théron, E. Brassat, C. Vaury, History of the discovery of a master locus
744 producing piRNAs: the flamenco/COM locus in *Drosophila melanogaster*. *Frontiers Genetics* 5,
745 257 (2014).
- 746 76. R. Kofler, Dynamics of Transposable Element Invasions with piRNA Clusters. *Molecular*
747 *Biology and Evolution* 36, 1457–1472 (2019).
- 748 77. A. and T. Péliesson, About the origin of retroviruses and the co-evolution of the gypsy
749 retrovirus with the *Drosophila* flamenco host gene. 29–37 (1997).
- 750 78. C. Duc, *et al.*, Trapping a somatic endogenous retrovirus into a germline piRNA cluster
751 immunizes the germline against further invasion. *Genome Biol* 20, 127 (2019).

- 752 79. Y. Luo, P. He, N. Kanrar, K. F. Toth, A. Aravin, Maternally inherited siRNAs initiate piRNA
753 cluster formation <https://doi.org/10.1101/2022.02.08.479612>.
- 754 80. R. Kofler, piRNA Clusters Need a Minimum Size to Control Transposable Element
755 Invasions. *Genome Biology and Evolution* 12, 736–749 (2020).
- 756 81. F. K. Teixeira, *et al.*, piRNA-mediated regulation of transposon alternative splicing in the
757 soma and germ line. *Nature* 552, 268–272 (2017).
- 758 82. V. V. Kapitonov, J. Jurka, Molecular paleontology of transposable elements in the
759 *Drosophila melanogaster* genome. *Proc National Acad Sci* 100, 6569–6574 (2003).
- 760 83. N. D. Singh, D. A. Petrov, Rapid Sequence Turnover at an Intergenic Locus in *Drosophila*.
761 *Mol Biol Evol* 21, 670–680 (2004).
- 762